Towards catheter pose estimation and data-based catheter steering

Bingbin Yu*, Abraham Temesgen Tibebu*, Jan Hendrik Metzen*,†
*Robotics Research Group, University of Bremen
†Robotics Innovation Center, German Research Center for Artificial Intelligence (DFKI GmbH)
Robert-Hooke-Str. 1, D-28359 Bremen, Germany
Email: Bingbin.Yu@uni-bremen.de

***Abstract*—Minimally invasive surgery (MIS) is an important approach for reducing injuries of the body, allowing faster recovery and healing, and is considered to be safer than open surgeries. Especially for the cardiovascular operations, catheter based diagnosis and therapy are becoming more popular these days. This paper presents an approach of tendon-driven catheter steering by using a joint probability density based catheter model. For tracking the catheter in a 3D rigid mockup, a Qualisys motion tracking system is used. The catheter steering is evaluated in simulation on a mesh generated from the real image data.**

I. Experimental Setup

The setup used for pose estimation of ablation catheter is shown in Figure 1. An RFA tendon-driven ablation catheter (EndoSense SA) is used which is placed inside a 3D rigid aorta mock-up. Due to the light reflection and refraction, optical tracking of the objects inside the plastic mock-ups are difficult. Moreover, self-occlusion is another challenge of the object tracking for the normal stereo camreas. Therefore, a near infrared motion tracking system is used: five Qualisys Oqus-300 near infrared cameras are placed around the mock-up and six reflective markers are attached on the catheter. Since the plastic mock-up is almost transparent for the near infrared cameras, the system detects the markers more effectively and the self-occlusion problem can be solved by increasing the number of the cameras.

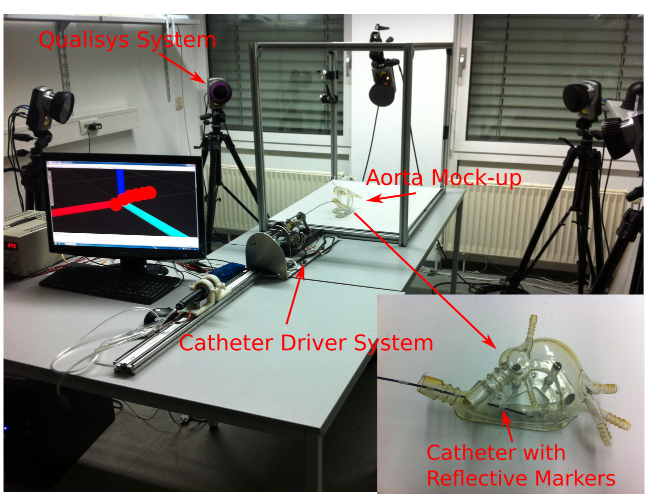

Fig. 1. Visualization of the experimental setup used for pose estimation of catheter with reflective markers inside 3D aorta mock-up

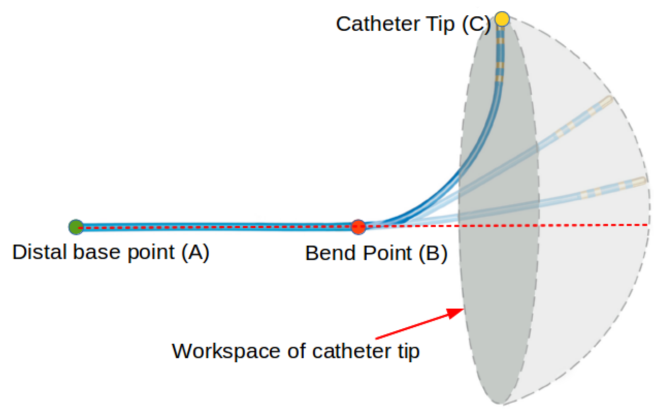

Fig. 2. The catheter steering mechanism and the corresponding bowl shaped catheter tip workspace.

II. Method

Due to the compliance of the catheter material and to unknown internal friction and associated internal load, the precise modelling of the tendon-driven catheter is still challenging and being studied by a number of groups, e.g. by Kesner et al. [1]. We provide a data-driven method for the position control of the catheter distal section that does not require the internal information of the ablation catheter.

Figure 2 illustrates the rotate and bend actions of a catheter distal section as well as the reachable position (workspace) of the catheter tip. The yellow, red and green points represent the catheter tip $\mathbf{C}$, bending point $\mathbf{B}$ and distal base point $\mathbf{A}$ respectively. The red dash line is the rotation axis of the catheter. Bending the catheter distal section in one direction, the trajectory of the catheter tip is an arc curve. According to the rotational symmetry, the shapes of the bended catheter distal section are the same in any rotation angle. Therefore, learning the catheter shape by applying the bend and rotate actions, the workspace of the catheter tip can be represented as a bowl shape surface, the shaded surface drawn in Figure 2.

During training, the joint probability distribution (JPD) [2] is learned:

$$p(\boldsymbol{\alpha_t}, \boldsymbol{\theta_t}, \boldsymbol{r_t}, \boldsymbol{d_t}) \quad (1)$$

There are four component in the training data. $\boldsymbol{\alpha}_t$ is the current shape of the catheter distal section, which is com-

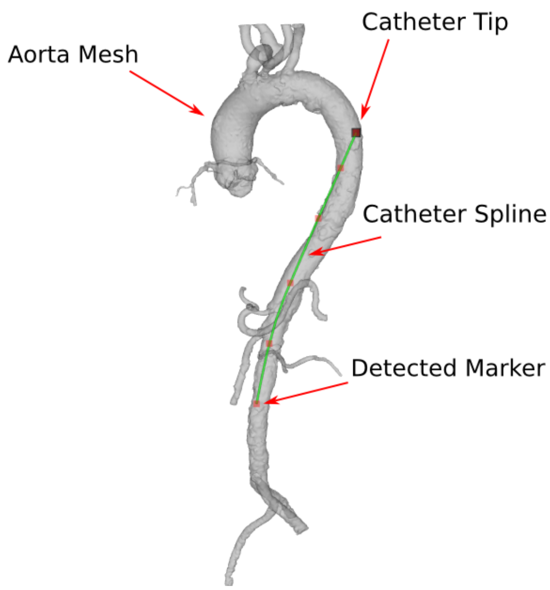

Fig. 3. The pose estimation using Qualisys system: Catheter spline is shown in green, all six of the reflective markers are shown with red dot.

posed by the positions of catheter interpolated knots, includes catheter tip point, catheter base point and catheter bend point. $\boldsymbol{\theta}_t$ represents the current bending angle of the catheter, $\boldsymbol{r}_t$ represents the current rotation angle of the catheter and $\boldsymbol{d}_t$ is the current push distance of the catheter handle. By applying the actions of bend and rotate, the next state of the catheter and the applied actions can be learned as well. Therefore, the JPD model is represented:

$$p(\boldsymbol{\alpha_{t+1}}, \boldsymbol{\theta_{t+1}}, \boldsymbol{r_{t+1}}, \boldsymbol{d_{t+1}}, \boldsymbol{\alpha_t}, \boldsymbol{\theta_t}, \boldsymbol{r_t}, \boldsymbol{d_t}, \boldsymbol{\delta_d}, \boldsymbol{\delta_r}) \quad (2)$$

Since the tendon-driven catheter is used, the bend action is represented by a displacement of the catheter handle $\boldsymbol{\delta_d}$ and $\boldsymbol{\delta_r}$ represents rotate action.

In the test, based on the current catheter shape $\boldsymbol{\alpha}_t$ and the every avaliable actions $\boldsymbol{\delta}_d^*, \boldsymbol{\delta}_r^*$, the workspace of the catheter tip can be estimated based on the model.

$$\mathbb{E}\left[\boldsymbol{p}_{t+1}^* | \boldsymbol{\alpha}_t, \boldsymbol{\theta}_t, \boldsymbol{r}_t, \boldsymbol{d}_t, \boldsymbol{\delta}_d^*, \boldsymbol{\delta}_r^*\right] \quad (3)$$

$\boldsymbol{p}_{t+1}^*$ is the workspace of the catheter tip. Therefore, The crossing point between the predefined trajectory and catheter tip workspace can be calculated as the reference position and the corresponding actions are the actions for steering the catheter. Further details are given by Yu et al. [3].

III. Results

In order to register the optical detected catheter into the simulated aorta mock-up, seven reflective markers are attached on the feature positions of 3D real aorta mock-up. By registering the detected feature points from real aorta mock-up to the virtual aorta mock-up in simulation, the catheter pose can be presented in the simulation enviroment as Figure 3 shows. The six reflective markers which are attached on the ablation catheter are detected and presented as the red dots in simulation. The green curve is the catheter shape which is calculated by the B-spline curve fitting method. The accuracy of the system is evaluated by moving two rigid markers in the testbed area, the distance between these two markers is fixed to 30cm. The standard deviation of the estimated distance and the real distance in 720 different positions reaches $0.4213mm$.

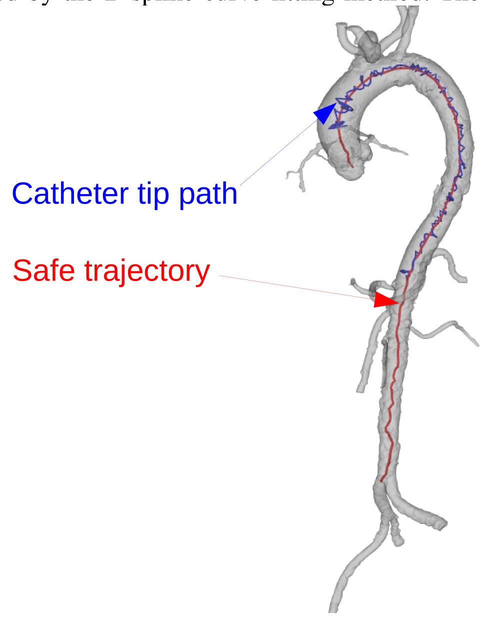

Fig. 4. The result of the catheter trajectory following experiment. The red curve represents the planned trajectory for the catheter and the blue curve is the followed path of the catheter tip.

For evaluating the catheter steering, a trajectory following experiment is conducted by using a catheter simulator. The simulator includes both a 3D aorta mesh representing the enviroment and a simulated catheter. For reducing the risk of catheter steering in the cardiovascular system, a trajectory for the catheter tip in the aorta main branch is planned, which keeps largest distance to the detected calcification areas from the real preoperative images. The catheter inserts into the simulated aorta with 2mm translation steps, based on the catheter steering algorithm, the catheter tip is steered towards the trajectory after each insertion step. Figure 4 shows the planned trajectory and the catheter tip position during the trajectory following test. The mean Euclidean distance from the catheter tip to the trajectory is 4.09mm.

For future works we will focus on realizing the catheter trajectory following in a real 3D experimental setup (shown in Figure 1), in which the catheter will be tracked by the Qualisys system.

References

[1] S. Kesner and R. Howe, "Position control of motion compensation cardiac catheters," in *IEEE TRANSACTIONS ON ROBOTICS*, vol. 27, no. 6, December 2011.

[2] M. Edgington, Y. Kassahun, and F. Kirchner, "Using joint probability densities for simultaneous learning of forward and inverse models," in *IEEE IROS International Workshop on Evolutionary and Reinforcement Learning for Autonomous Robot Systems*, N. T. Siebel and J. Pauli, Eds., 10 2009, pp. 19–22.

[3] B. Yu, A. Tibebu, Y. Kassahun, F. Bernhard, and E. B. Vander Poorten, "Towards learning-based catheter distal section steering," in *Proceedings of the 4rd Joint Workshop on New Technologies for Computer/Robot Assisted Surgery (CRAS)*, 2014, pp. 167–170.